

# Magnetic levitation properties of single- and multi-grain YBCO bulk superconductors

C.-J. Kim<sup>\*a</sup>, A. Y. Yang<sup>b</sup>, S. H. Lee<sup>b</sup>, and B.-H. Jun<sup>a</sup>

<sup>a</sup>Korea Atomic Energy Research Institute, Korea

<sup>b</sup>Sunmoon University

(Received 14 June 2022; revised or reviewed 22 September 2022; accepted 23 September 2022)

## Abstract

Single-grain (c-normal or c-parallel) and multi-grain YBCO superconductors were prepared by a melt growth process with/without seeding. The magnetic levitation force and trapped magnetic field at liquid N<sub>2</sub> temperature (77 K) of the YBCO superconductors were investigated. Samples for the levitation force measurement were zero-field cooled (ZFC) to 77 K, and samples for trapped field measurement were field-cooled (FC) using Nd magnets. As for the magnetic levitation force, the c-normal, single grain sample showed the largest value, whereas the multi-grain sample showed the lowest value. The trapped magnetic field of the c-normal and c-parallel single-grain samples was 4-5 times that of the multi-grain sample. In addition, as the external magnetic field (the number of magnets) increased, the both properties increased proportionally. These results were explained in terms of the orientation dependence of the levitation forces and the magnetic field trapping capability of the YBCO superconductor.

*Keywords:* YBCO, superconductor, magnetic levitation force, trapped magnetic field, single-grain, multi-grain, orientation

## 1. INTRODUCTION

The high-temperature YBa<sub>2</sub>Cu<sub>3</sub>O<sub>7-d</sub> superconductor (hereinafter YBCO) has a superconducting transition temperature ( $T_c$ ) of 93 K [1], which is higher than the boiling point (77 K) of liquid nitrogen (LN<sub>2</sub>) that is a cheaper refrigerant. Much effort has been done for the practical use of YBCO. For this, it is necessary to increase the critical current density ( $J_c$ ) of YBCO at the magnetic fields. Melt growth process utilizing incongruent melting and slow cooling through the peritectic temperature is one of effective ways that increase the  $J_c$  of YBCO. When YBCO is manufactured by the melt growth processing, a very large grain of several cm grow from the melt [2-5]. The large grain YBCO superconductor showed very high  $J_c$  even at magnetic fields of several tesla (T) [2-4].

The large-grain YBCO bulk superconductor can be used a part of the magnetic levitation devices (e. g, active bearings of flywheel energy storage system [6]) that utilize the strong repulsive force between the superconductor and the permanent magnet. In addition to the large levitation force, a very large magnetic field can be trapped inside the superconductor. A magnetic field of more than 15 T can be stored in the superconductor at 20 K [7-9]. The large grain superconducting can be used as a bulk magnet in a superconducting magnetic separator [10].

The magnetic levitation force of the superconductor depends on the material factors such as  $J_c$  and grain size of YBCO, and the magnetic strength of a permanent magnet [11-14]. When the larger magnetic field is applied to the superconductor, the repulsive force between the

superconductor and magnet is large. In addition, the strength of the magnetic levitation force depends on the crystal orientation of YBCO. This is because the current flow along the direction normal to the c-axis of YBCO is much larger than that parallel to the c-axis [5, 14]. For the development of the superconductor energy storage device, therefore, it is necessary to understand the superconductor-magnet interaction as well as the magnetic levitation properties of the superconductor.

In this study, YBCO samples of single-grain YBCO samples whose growth direction is normal or parallel to the c-axis of YBCO and multiple grains were fabricated. The magnetic levitation properties of the three YBCO samples were compared.

## 2. EXPERIMENTS

### 2.1. Sample preparation

The YBCO bulk superconductors used in this study were prepared by the seeded melt growth process. 0.3 mole of Y<sub>2</sub>O<sub>3</sub> and 1 wt. % of CeO<sub>2</sub> were added to YBCO powder to refine the Y211 particles [17], which enhance the flux pinning capacity. The powder mixture was put into a square mold and pressed into a compact with a side length of 40 mm. The growth direction of YBCO was controlled using SmBCO seeds with various crystallographic orientations. The c-normal seed or c-parallel seed was used for the fabrication of single grain YBCO samples and no seed was used for the multi-grain sample. The YBCO powder compacts with/without seed were put into a box furnace and a melt process heat treatment was applied to

\* Corresponding author: cjkim2@kaeri.re.kr

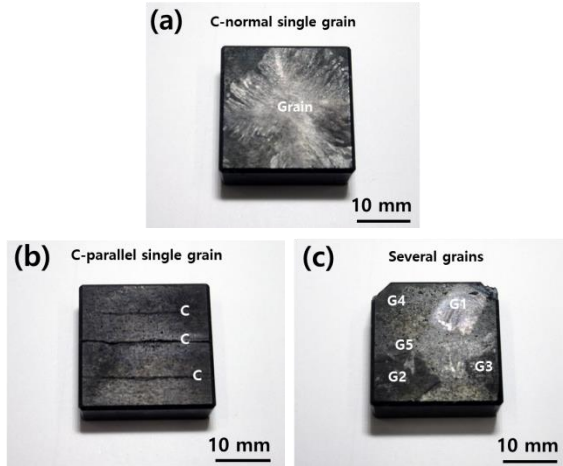


Fig. 1. Single grain sample with (a) c-normal, (b) c-parallel orientation, and (c) multi-grain sample with random orientation.

the compacts. The applied heat treatment profiles are documented in detail in other papers [18].

Figure 1 shows the top surface of single-grain YBCO sample with (a) c-normal orientation, (b) c-parallel orientation, and (c) multi-grain sample with random orientation. The initial side length of the powder compact was 40 mm. After the melting process, the side length was reduced to 30 mm due to the densification during the heat treatment.

As can be seen in Fig. 1(a), one large YBCO grain of 25 mm or more was grown on the top surface of the sample (a). The grain orientation is normal to the c-axis of YBCO. Unlike sample (a), a large grain grew parallel to the c-axis of YBCO on the top surface of sample (b). Several lines perpendicular to the top surface (see the lines marked by c) are observed, which are cracks formed on the a-b plane of YBCO due to the stress of orthorhombic-to-tetragonal phase transition during oxygen heat treatment [19, 20]. The cracks developed throughout the sample indicate that the YBCO grain grew to one direction in entire top surface. On the other hand, several YBCO grains are observed to grow in random orientations on the top surface of the sample (c) (see the regions marked by G1-G5 in Fig. 1(c)). In our previous work [13], we analyzed the crystal orientation of the YBCO growth surface by X-ray diffraction method. With reference to the analysis, the crystal orientation of the samples used in this study could be easily predicted.

## 2.2. Magnetic levitation force

The magnetic levitation force of YBCO samples at 77 K was measured by zero-field cooling (ZFC) method. A sample was placed in a cooling bowl, and LN2 was poured into the sample, and held for 1-2 minutes (see Fig. 2). After cooling was completed, the permanent magnet was brought close to the superconductor. The repulsive force ( $F$ ) between the superconductor and magnet was estimated using the scale (weighing device) placed under the sample holder and is plotted as a function of distance ( $d$ ). For the magnetic force measurement, an Nd magnet with a diameter of 20 mm and a thickness of 10 mm was used, and the number of magnets was changed to increase the

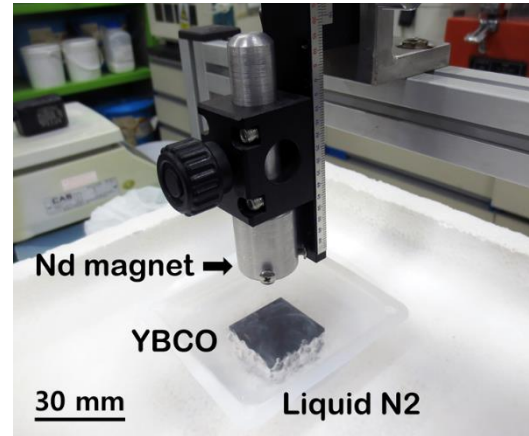


Fig. 2. Superconducting magnetic levitation force measuring device.

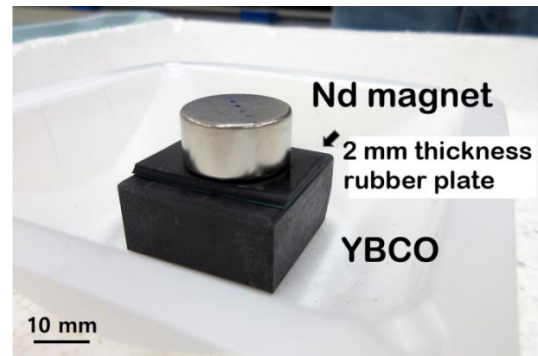


Fig. 3. Arrangement of an Nd magnet, gap-making rubber plate and YBCO for field cooling experiment.

magnetic force. When one Nd magnet was used, the surface magnetic force ( $H$ ) was 378 mT, and when the number of magnets was increased to two and three, the magnetic field was 457 mT and 482 mT, respectively.

## 2.3. Trapped magnetic field

To measure the magnetic field trapped in the YBCO superconductor, samples was field-cooled (FC). For this, a superconductor, gap-making rubber plate, and Nd magnet were arranged as shown in Fig. 3. A 2 mm thick rubber plate was inserted between the superconductor and the magnet. Therefore, the measured magnetic field is the value when the gap distance is 2 mm. The reason for inserting a rubber plate between the YBCO and the magnet is to make it easier to separate the magnet from the superconductor after LN2 cooling. After placing a permanent magnet on the superconductor, LN2 was poured into the superconductor. When the superconductor was completely cooled, the rubber plate was removed and the magnet was separated from the superconductor. The magnetic field of the top surface of YBCO was measured using a gauss meter.

# 3. RESULTS AND DISCUSSION

## 3.1. Magnetic levitation force

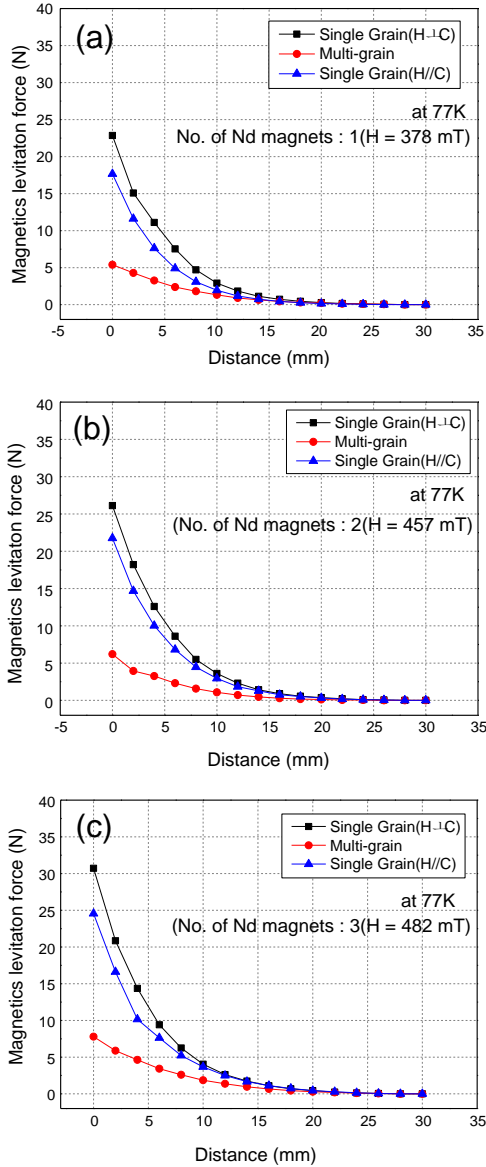


Fig. 4. Force-distance ( $F$ - $d$ ) curves at 77 K of YBCO samples measured using (a) one, (b) two, and (c) three magnets.

Figure 4 shows the force-distance ( $F$ - $d$ ) curves at 77 K of YBCO samples measured using (a) one, (b) two, and (c) three Nd magnets. As can be seen in Fig. 4(a), the repulsive force ( $F$ ) between the YBCO samples and the magnet appears at about 30 mm. The surface magnetic force of a single Nd magnet is 378 mT. As the distance ( $d$ ) between the superconductor and the magnet decreases,  $F$  increases rapidly. This is because the magnetic force ( $H$ ) of a permanent magnet is inversely proportional to the distance ( $d$ ) squared ( $H = A/d^2$  [21], where  $A$  is constant).

For the multi-grain sample composed of several grains, a maximum repulsive force ( $F_{max}$ ) at  $d=1$  mm is 5.4 N. On the other hand,  $F_{max}$ s of the c-normal and c-parallel single-grain sample were 17.6 N and 22.8 N, respectively, which were relatively higher than the multi-grain samples. Even in the single-grain samples,  $F$  of the c-normal sample is higher than that of the c-parallel sample, because the highest current flows in the c-normal direction in the YBCO crystal [15, 16].

When  $F$  of the same YBCO samples was measured using two magnets, an  $F$ - $d$  curve similar to Fig. 4(a) could be obtained. An increase in the number of magnets increases the  $H$  value of the magnet, which leads to an increase in  $F$  of the superconductors. When two magnets are superimposed,  $H$  of the magnet is 457 mT, which is 17% higher than the  $H$  of one magnet, 378 mT.  $F_{max}$  of the c-normal sample is 26.1 N, which is 12% higher than 22.8 N when using one magnet.

As can be seen in Fig. 4(c), even when three magnets are used ( $H=482$  mT),  $F$ s of samples increase over the entire  $d$  range.  $F_{max}$  of the multi-grain sample and the c-normal sample were 7.8 N and 30.7 N, respectively. In this study, when the magnetic force of the magnet increased from 378 mT to 482 mT (one to three magnets),  $F_{max}$  of the multi-grain sample increased from 5.39 N to 7.8 N, and  $F_{max}$  of the c-normal sample increased from 22.8 N to 30.7 N. These values correspond to an increase in repulsive force of about 40%. The repulsive force acting between the superconductor and the permanent magnet is one of the factors that determine the energy storage capacity of the superconducting magnetic levitation device. The results of this study indicate that a magnet with high magnetic force should be used to levitate large weight (to storage large energy).

### 3.2. Trapped magnetic field

Figure 5 shows the magnetic distribution maps of the top surface of (a) c-normal, (b) c-parallel single-grain samples and (c) multi-grain samples. These are field maps measured on superconducting samples that have been field-cooled to 77 K using magnets one, two and three magnets. As shown in Fig. 5(a), in the field map of the c-normal sample, there is a peak at the center, and the strength of the trapped field gradually weakens toward the edge of the sample. This is a typical map that appears in a single crystal. Also, as the number of magnets used increases (increasing the applied magnetic field), the magnetic field trapped in the sample increases proportionally. For  $H = 378$  mT,  $H = 457$  mT and  $H = 482$  mT, the magnetic fields trapped on the top surface were 224 mT, 239 mT and 253 mT respectively.

Figure 5(b) shows the magnetic field distribution on the top surface of the c-parallel sample. There are two peaks in the center of the curve, and the maximum trapped field is 250 mT. The valley located between the two central peaks indicates a discontinuity of the superconducting grain at the center. The trapped magnetic field at the valley is 200 mT. Grain boundaries, continuous non-superconducting inclusions such as a liquid layer, and cracks are possible causes of the discontinuity in superconducting grains [18, 22]. In this study, the crack observed in Fig. 1(b) is thought to be the cause of the discontinuity. Similar to the result observed in Fig. 5(a), the strength of the magnetic field trapped on the surface is proportional to the number of permanent magnet used during cooling (applied magnetic field). As the external magnetic field increases, the magnetic field trapped in the superconductor increases.

Figure 5(c) shows the magnetic field distribution of the multi-grain sample. There are also two peaks in this curve, and the peak strength on the left is relatively larger than

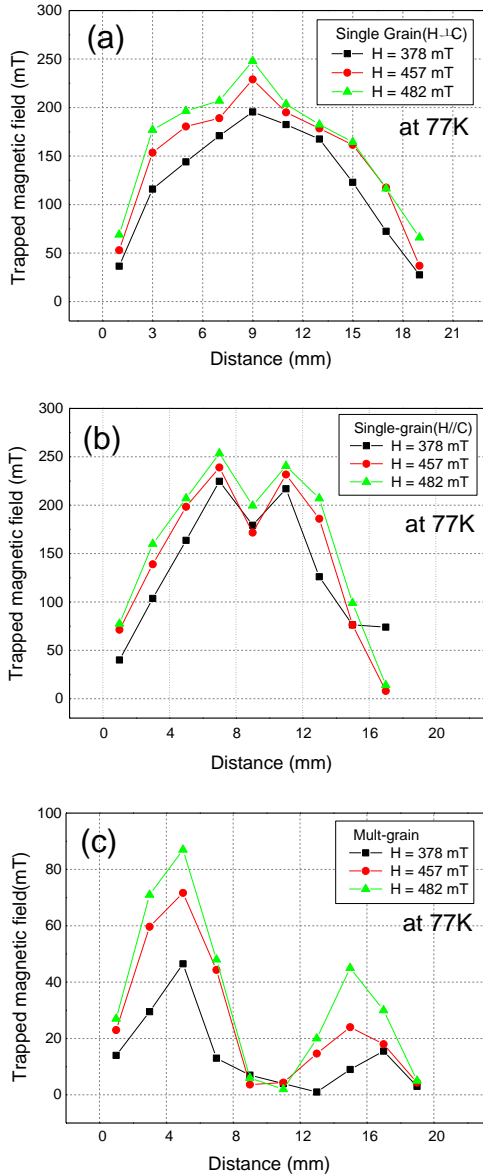


Fig. 5. Magnetic distribution maps of the top surface of (a) c-normal (b) c-parallel single-grain sample, and (c) multi-grain sample.

that on the right. The trapped magnetic fields of the two peaks are 90 mT and 50 mT, respectively, and the magnetic field trapped between the two peaks is close to zero (center position of the sample). This is compared with the magnetic field (200 mT) in the central valley shown in the c-parallel sample in Fig. 5(b). Another noteworthy point is that the maximum trapped field of this sample is very small, about half that of sample (a) or sample (b). The magnetic field trapped in the superconductor is dependent on  $J_c$  of the superconductor and the grain size [16]. Since all samples were prepared under the same process conditions,  $J_c$  of the samples will be similar. Then, the difference between the samples is the grain size. Samples (a) and (b) are single-grain and their grain sizes are about 30  $\mu\text{m}$ , whereas sample (c) is composed of several grains which varies from 1  $\mu\text{m}$  to several  $\mu\text{m}$ . Therefore, it is thought that the grain size caused the difference in the trapped magnetic field between the samples. The maximum trapped magnetic field of each sample is summarized in Fig.

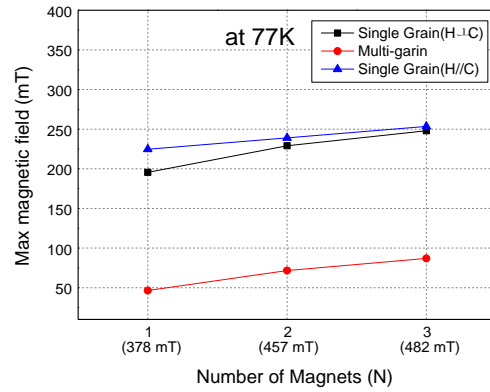


Fig. 6. Maximum trapped magnetic field of a c-normal, c-parallel and multi-grain sample as a function of the external magnetic field (number of magnets).

6 as a function of the external magnetic field (number of magnets).

The magnetic levitation force and trapping flux of YBCO depend on the material properties. In the case of a use of a magnet of several thousand Gauss, the magnetic levitation force decreases rapidly when the thickness of the YBCO superconductor is 8 mm or less [12, 13]. In addition, as confirmed in this study and other studies, the single grain samples without grain boundaries show better performance than the multi-grain sample. In particular, the existence of discontinuity such as grain boundaries and cracks causes a significant decrease in magnetic levitation properties [18, 22]. Also, the homogeneity of the microstructure of YBCO (existence of pores or oxygen deficiency) affected the magnetic properties [14]. Among the various variables the grain size is thought to be the most important factor that decides the magnetic levitation properties of the superconductor because the shielding current generated by the external magnetic field is limited inside the grain.

Figure 7 shows a superconducting magnetic bearing used in rotating devices. As shown in this figure, a permanent magnet is levitated above the YBCO superconductor cooled with liquid nitrogen. A repulsive force and an attractive force act simultaneously between the two objects. Superconducting bearings are used to increase energy storage efficiency by reducing friction between mechanical parts. To store large energy in a superconducting energy storage device, the repulsive force between the permanent magnet and the superconductor should be large. For this, the current carrying capability of the superconductor needs to be improved and a permanent magnet with high magnetic force should be used.

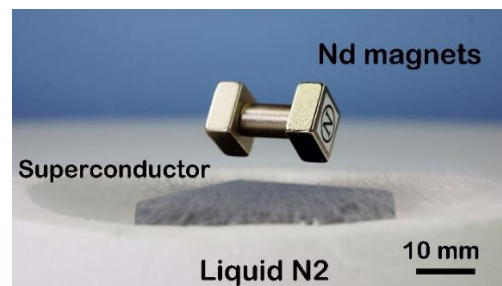


Fig. 7. Superconducting magnetic bearing used in a rotating machine.

#### 4. CONCLUSIONS

In this study, the magnetic levitation force and trapped magnetic field at 77 K of single- and multi-grain YBCO superconductors were investigated. The single grain sample (c-normal) showed the largest levitation force, whereas the multi-grain sample showed the lowest. As the external magnetic field increased, the magnetic levitation force increased. In addition to the magnetic levitation force, the trapped magnetic fields of single-grain samples (c-normal and c-parallel) were higher than that of the multi-grain sample. This is attributed to the orientation dependence of  $J_c$  of the YBCO superconductor, the difference in grain size and magnetic field trapping capability of the superconducting grain. The result of this study is expected to be used for the development of superconducting energy storage devices utilizing the superconductor-magnet interaction.

#### ACKNOWLEDGMENTS

This work was supported by the National Research Foundation Grant (NRF-2020M2D8A2047959) funded from Ministry of Science and ICT(MSIT) of Republic of Korea.

#### REFERENCES

- [1] M. K. Wu, J. R. Ashburn, C. J. Torng, P. H. Hor, R. L. Meng, L. Gao, Z.J. Huang, Y. Q. Wang, and C.W. Chu, "Superconductivity at 93 K in a New Mixed-Phase Y-Ba-Cu-O Compound System at Ambient Pressure," *Phys. Rev. Lett.*, vol. 58, pp. 908-910, 1988.
- [2] S. Jin, T. H. Tiefel, R. C. Sherwood, R. B. van Dover, M. E. Davis, G.W. Kammlott, and R. A. Fastnacht, "Melt-textured growth of polycrystalline  $YBa_2Cu_3O_{7-\delta}$  with high transport  $J_c$  at 77 K," *Phys. Rev. B* 37, pp. 7850-7853, 1988.
- [3] K. Salama, V. Selvamanickam, L. Gao, and K. Sun, "High current density in bulk  $YBa_2Cu_3O_x$  superconductor," *Appl. Phys. Lett.*, vol. 54, no. 23, pp. 2352-2354, 1989.
- [4] M. Murakami, M. Morita, K. Doi, and K. Miyamoto, "A New Process with the Promise of High  $J_c$  in Oxide Superconductors," *Jpn. J. Appl. Phys.*, vol. 28, no.7, pp. 1189-1194, 1989.
- [5] C. J. Kim and G. W. Hong, "Defect formation, distribution and size reduction of  $Y_2BaCuO_5$  in melt-processed YBCO superconductors," *Supercond. Sci. Technol.*, vol. 12, pp. R27-R41, 1999.
- [6] M. Strasik, J. R. Hull, J. A. Mittleider, J. F. Gonder, P. E. Johnson, K. E. McCrary and C. R. McIver, "An overview of Boeing flywheel energy storage systems with high-temperature superconducting bearings," *Supercond. Sci. Technol.* vol. 23, p. 034021, 2010.
- [7] M. Tomita, and M. Murakami, "High-temperature superconductor bulk magnets that can trap magnetic fields of over 17 tesla at 29 K," *Nature*, vol. 421, pp. 517-520, 2003.
- [8] G. Fuchs, P. Schätzle, G. Krabbes, S. Gruss, P. Verges, K-H. Müller and J. Fink, "Trapped magnetic fields larger than 14 T in bulk  $YBa_2Cu_3O_{7-x}$ ," *Appl. Phys. Lett.*, vol. 76, pp. 2107-2109, 2000.
- [9] T. Oka, H. Kanayama, S. Fukui, J. Ogawa, T. Sato, M. Oozumi, T. Terasawa, Y. Itoh, and R. Yabuno, "Application of HTS bulk magnet system to the magnetic separation techniques for water purification," *Physica C*, vol. 468, no. 15-20, pp. 2128-2132, 2007.
- [10] J. H. Durrell., A. R. Dennis., J. Jaroszynski, M. D. Ainslie, K. G. B. Palmer, Y-H. Shi, A. M. Campbell, J. Hull, M. Strasik, E. Hellstrom, and D. A. Cardwell, "A Trapped Field of 17.6 T in Melt-Processed, Bulk Gd-Ba-Cu-O Reinforced with Shrink-Fit Steel," *Supercond. Sci. Technol.*, vol. 27, pp. 082001, 2014.
- [11] M. Murakami, T. Oyama, H. Fujimoto, T. Taguchi, S. Gotoh, Y. Shiohara, N. Koshizuka, and S. Tanaka, "Large Levitation Force due to Flux Pinning in  $YBaCuO$  Superconductors Fabricated by Melt-Powder-Melt-Growth Process," *Jpn. J. Appl. Phys.*, vol. 29, no. 11, pp. L1991-L1994, 1990.
- [12] Y. S. Lee, H. S. Park, I. H. Kuk, G. W. Hong, and C. J. Kim, "Levitation force of melt-textured single- and multi-domain  $YBaCuO$  superconductors," *Korean J. Mater. Res.*, vol. 8, pp. 105-113, 1998.
- [13] Y. Jung, S. J. Go, H. T. Joo, Y. J. Lee, S.-D. Park, B.-H. Jun, and C.-J. Kim, "Orientation and thickness dependence of magnetic levitation force and trapped magnetic field of single grain  $YBa_2Cu_3O_{7-y}$  bulk superconductors," *Prog. Supercond. Cryogen.*, vol. 19, no. 1, pp. 30-35, 2017.
- [14] S.-D. Park, H.-W. Park, B.-H. Jun, and C.-J. Kim, "Effects of artificial holes in very large single-grain  $Y_{1.5}Ba_2Cu_3O_{7-y}$  bulk superconductors," *Prog. Supercond. Cryogen.*, vol. 19, No. 3, pp.27~32, 2017.
- [15] A. Xu, J. J. Jaroszynski, F. Kametani, Z. Chen, D. C. Larbalestier, Y. L. Viouchkov, Y. Chen, Y. Xie, and V. Selvamanickam, "Angular dependence of  $J_c$  for YBCO coated conductors at low temperature and very high magnetic fields," *Supercond. Sci. Technol.*, vol. 23, pp. 014003 (7pp), 2010.
- [16] M. Murakami, *Melt processed high-temperature superconductors*, 1<sup>st</sup> ed., Chapter 6, Singapore: World Scientific, 1992, pp. 127-131.
- [17] Chan-Joong Kim, Il-Hyun Kuk, Gye-Won Hong, Tae-Hyun Sung, Sang-Chul Han, and Jin Joong Kim, "CeO<sub>2</sub> as a growth inhibitor of  $Y_2BaCuO_5$  in a  $Ba_3Cu_5O_x$  liquid phase," *Materials Letters*, vol. 34, pp. 392-397, 1998.
- [18] Y. A. Jee, C.-J. Kim, T.-H. Sung, and G.-W. Hong, "Top seeded melt growth of Y-Ba-Cu-O superconductor with multiseeding," *Supercond. Sci. Technol.*, vol. 13, pp. 195-201, 2000.
- [19] C. J. Kim, K. B. Kim, I. H. Kuk, G. W. Hong, Y. S. Lee, and H. S. Park, "Microstructure change during oxygen annealing and the effect on the levitation force of melt-textured Y-Ba-Cu-O superconductors," *Supercond. Sci. Technol.*, vol. 10, pp. 947-954, 1997.
- [20] C. J. Kim, Y. S. Lee, H. S. Park, I. H. Kuk, T. H. Sung, J. J. Kim, and G. W. Hong, "Oxidation induced formation of a-b planar defects in melt-textured  $YBa_2Cu_3O_{7-y}$  containing  $Y_2BaCuO_5$  inclusions," *Physica C*, vol. 276, pp. 101-108, 1997.
- [21] [https://en.wikipedia.org/wiki/Force\\_between\\_magnets](https://en.wikipedia.org/wiki/Force_between_magnets).
- [22] Zigang Deng, Mitsuru Izumi, Motohiro Miki, Keita Tsuzuki, Brice Felder, Wei Liu, Jun Zheng, Suyu Wang, Jiasu Wang, Uta Floegel-Delor, and Frank N. Werfel, "Trapped Flux and Levitation Properties of Multiseeded YBCO Bulks for HTS Magnetic Device Applications-Part II: Practical and Achievable Performance," *IEEE Trans. Appl. Supercond.*, vol. 22, pp. 6800210, 2012.